# Thermodynamically Consistent discretisation of a Thermo-Hydro-Mechanical model

Jérome Droniou, Mohamed Laaziri, Roland Masson

# Thermodynamically Consistent discretisation of a Thermo-Hydro-Mechanical model

Jérome Droniou[1], Mohamed Laaziri[2], and Roland Masson[3]

[1] School of Mathematics, Monash University, Victoria 3800, Australia,
jerome.droniou@monash.edu,
[2] Université Côte d'Azur, Inria, CNRS, Laboratoire J.A. Dieudonné, team Coffee, France,
mohamed.laaziri@univ-cotedazur.fr,
[3] Université Côte d'Azur, Inria, CNRS, Laboratoire J.A. Dieudonné, team Coffee, France,
roland.masson@univ-cotedazur.fr

**Abstract.** We consider in this work a Thermo-Hydro-Mechanical (THM) model coupling the non-isothermal single phase flow in the porous rock and the linear thermo-poro-elasticity. This type of models plays an important role in several applications such as e.g. the hydraulic stimulation of deep geothermal systems, or the risk assessment of induced sismicity in CO2 storages. Compared with the isothermal case, the thermal coupling induces additional difficulties related in particular to the nonlinear convection term. Starting from the pioneer work of Coussy [2], we introduce a thermodynamically consistent discretisation of the THM coupled model which naturally leads to a discrete energy estimate. Our approach applies to a large class of Finite Volume schemes for the flow and energy equations but to fix ideas we consider the Hybrid Finite Volume (HFV) discretisation [3]. It is combined with a conforming Galerkin approximation of the mechanics. Our methodology accounts for a wide range of thermodynamical single phase fluid model and of thermo-poro-elastic parameters, as well as for diffusive or convective dominated energy transport. The efficiency of our approach is assessed on a 2D analytical test case using the HFV scheme for the non-isothermal flow and a $\mathbb{P}_2$ Finite Element method for the mechanics.

**Keywords:** Thermo-poro-mechanics, energy estimates, thermodynamically consistent discretization, finite volume

## 1 Continuous model

We consider a Thermo-Poro-Mechanical (THM) model under the hypothesis of small perturbations for the skeleton accounting for small transformations, displacement and variations of porosity [2]. Linear isotropic thermo-poro-elastic constitutive laws are considered for the skeleton assuming small variations of temperature around the reference temperature $T_0$. The Darcy law is used for the fluid velocity and the Fourier law for the thermal conduction. Thermal equilibrium is assumed between the fluid and the skeleton, and the fluid dissipation is neglected on an assumption of small Darcy velocities. The mechanical inertial term is modelled using the freezed specific average fluid -

rock density $m_0$. Following [2], the resulting THM model is

$$\partial_t(\rho\overline{\phi}) + \mathrm{div}(\rho\overline{\mathbf{V}}) = h_m \quad \text{in } (0,\tau)\times\Omega, \tag{1a}$$

$$\partial_t(\overline{S}_s + \rho\overline{\phi}\overline{s}) + \mathrm{div}(\rho\overline{s}\overline{\mathbf{V}}) + \frac{1}{T_0}\mathrm{div}\overline{\mathbf{q}} = \frac{h_e}{\overline{T}} \quad \text{in } (0,\tau)\times\Omega, \tag{1b}$$

$$m_0\partial_t^2\overline{\mathbf{u}} - \mathrm{div}(\boldsymbol{\varpi}(\overline{\mathbf{u}},\overline{p},\overline{T})) = \mathbf{h} \quad \text{in } (0,\tau)\times\Omega, \tag{1c}$$

with

$$\overline{\mathbf{V}} = -\frac{\mathbb{K}}{\mu}\nabla\overline{p}, \quad \overline{\mathbf{q}} = -\lambda\nabla\overline{T}, \tag{1d}$$

$$\partial_t\overline{\phi} = b\partial_t(\mathrm{div}\overline{\mathbf{u}}) - 3\alpha_\phi\partial_t\overline{T} + \frac{1}{N}\partial_t\overline{p}, \tag{1e}$$

$$\partial_t\overline{S}_s = 3\alpha_s K_s\partial_t(\mathrm{div}\overline{\mathbf{u}}) - 3\alpha_\phi\partial_t\overline{p} + \frac{C_s}{T_0}\partial_t\overline{T}, \tag{1f}$$

$$\boldsymbol{\varpi}(\overline{\mathbf{u}},\overline{p},\overline{T}) = \boldsymbol{\varpi}^e(\overline{\mathbf{u}}) - b\overline{p}\,\mathbb{I} - 3\alpha_s K_s(\overline{T}-T_0)\mathbb{I}, \tag{1g}$$

$$\boldsymbol{\varpi}^e(\overline{\mathbf{u}}) = \frac{E}{1+\nu}\left(\mathfrak{e}(\overline{\mathbf{u}}) + \frac{\nu}{1-2\nu}(\mathrm{div}\overline{\mathbf{u}})\mathbb{I}\right). \tag{1h}$$

The primary unknowns of the model (1) are the fluid pressure $\overline{p}$, the fluid temperature $\overline{T}$ and the skeleton displacement field $\overline{\mathbf{u}}$. They are solutions of the nonlinear system of PDEs coupling the fluid mass conservation equation (1a), the total entropy conservation equation (1b), and the skeleton momentum balance equation (1c). The closure laws (1d)–(1h) define the Darcy velocity $\overline{\mathbf{V}}$, the conductive heat flux $\overline{\mathbf{q}}$, and account for the linear thermo-poro-elastic constitutive laws defining the porosity $\overline{\phi}$, the volumetric skeleton entropy $\overline{S}_s$ and the total stress tensor $\boldsymbol{\varpi}$ (from the effective stress tensor $\boldsymbol{\varpi}^e$). The parameters $E$ and $\nu$ are the effective Young modulus and Poisson coefficient, $N$ is the Biot modulus, $b$ the Biot coefficient, $K_s = \frac{(1+(d-2)\nu)E}{d(1+\nu)(1-2\nu)}$ is the bulk modulus, $d$ the space dimension, $3\alpha_s$ is the volumetric skeleton thermal dilation coefficient, $3\alpha_\phi$ is the volumetric thermal dilation coefficient related to the porosity, $C_s$ is the skeleton volumetric heat capacity, and $m_0$ is the average fluid skeleton specific density considered freezed at its initial value.

To simplify the presentation, the fluid is assumed incompressible with a constant specific density $\rho > 0$ , a constant dynamic viscosity $\mu > 0$, and the gravity terms are not considered. The fluid specific entropy $\overline{s}$ and internal energy $\overline{e}$ depend only on the temperature $\overline{T}$ and are such that $d\overline{e} = \overline{T}d\overline{s}$. Note that the methodology presented below readily extends to the case with gravity terms, general fluid thermodynamics, and $\overline{p},\overline{T}$ dependent viscosity.

To prepare the discretisation, we need to recast (1b). We have

$$\begin{aligned}\partial_t(\rho\overline{\phi}\overline{s}) + \mathrm{div}(\rho\overline{s}\overline{\mathbf{V}}) &= \rho\overline{\phi}\partial_t\overline{s} + \rho\overline{\mathbf{V}}\cdot\nabla\overline{s} + \overline{s}\underbrace{(\partial_t(\rho\overline{\phi}) + \mathrm{div}(\rho\overline{\mathbf{V}}))}_{=h_m \text{ by (1a)}} \\ &= \frac{\rho\overline{\phi}}{\overline{T}}\partial_t\overline{e} + \frac{1}{\overline{T}}\rho\overline{\mathbf{V}}\cdot\nabla\overline{e} + \overline{s}h_m,\end{aligned}$$

where we have used the relation $d\overline{e} = \overline{T} d\overline{s}$ in the second line. This leads to replacing (1b) with

$$\partial_t \overline{S}_s + \frac{\rho\overline{\phi}}{\overline{T}}\partial_t \overline{e} + \frac{1}{\overline{T}}\rho\overline{\mathbf{V}}\cdot\nabla\overline{e} + \frac{1}{T_0}\mathrm{div}\overline{\mathbf{q}} = \frac{h_e}{\overline{T}} - \overline{s}h_m. \tag{2}$$

To keep the presentation simple, we consider no-flow, no-energy flux and no-displacement boundary conditions.

## 2 Discretisation

Let $\mathscr{M}$ denote the set of cells, and $\mathscr{F}$ the set of faces of the mesh, with internal faces gathered in $\mathscr{F}^{\mathrm{int}}$ and boundary faces in $\mathscr{F}^{\mathrm{ext}}$. The subset $\mathscr{F}_K \subset \mathscr{F}$ denotes the set of faces of the cell $K \in \mathscr{M}$, and we denote by $\sigma = K|L$ the face between two cells $K, L$; the notation $\sigma = K|\cdot$ is used for a face $\sigma \in \mathscr{F}_K \cap \mathscr{F}^{\mathrm{ext}}$. For the pressure and temperature discretisation, we define the vector space of discrete unknowns

$$X_{\mathscr{D}} = \{v = ((v_K)_{K\in\mathscr{M}}, (v_\sigma)_{\sigma\in\mathscr{F}}) : v_K \in \mathbb{R} \text{ for all } K \in \mathscr{M},\, v_\sigma \in \mathbb{R} \text{ for all } \sigma \in \mathscr{F}\}.$$

We let $\nabla_{\mathscr{D}} : X_{\mathscr{D}} \to L^\infty(\Omega)^d$ be the HFV gradient reconstruction operator, and the cellwise constant function reconstruction operator $\Pi_{\mathscr{D}} : X_{\mathscr{D}} \to L^2(\Omega)$ is such that for all $v \in X_{\mathscr{D}}$ and all $K \in \mathscr{M}$, $(\Pi_{\mathscr{D}} v)_{|K} = v_K$. For the displacement field discretisation, we denote by $\mathbf{U}_{\mathscr{D}}$ a finite-dimensional subspace of $H^1_0(\Omega)^d$.

The HFV Darcy and Fourier fluxes are denoted respectively by $V_{K,\sigma}$ and $G_{K,\sigma}$ defined from $X_{\mathscr{D}}$ to $\mathbb{R}$ such that, for all $v, w \in X_{\mathscr{D}}$, all $K \in \mathscr{M}$ and $\sigma \in \mathscr{F}_K$,

$$\int_K \frac{\mathbb{K}}{\mu}\nabla_{\mathscr{D}} v \cdot \nabla_{\mathscr{D}} w = \sum_{\sigma\in\mathscr{F}_K} V_{K,\sigma}(v)(w_K - w_\sigma),$$

and

$$\int_K \frac{\lambda}{T_0}\nabla_{\mathscr{D}} v \cdot \nabla_{\mathscr{D}} w = \sum_{\sigma\in\mathscr{F}_K} G_{K,\sigma}(v)(w_K - w_\sigma).$$

Let the index $\sigma,+$ denote either $\sigma$ if no upwinding is used, or an upwind choice between $K$ and $L$ if $\sigma = K|L \in \mathscr{F}^{\mathrm{int}}$ and an upwind choice between $K$ and $\sigma$ if $\sigma = K|\cdot \in \mathscr{F}^{\mathrm{ext}}$. A key ingredient of the spatial discretisation that enables an energy estimate is the following discretisation of $\rho\overline{\mathbf{V}}\cdot\nabla\overline{e} = \mathrm{div}(\rho\overline{e}\overline{\mathbf{V}}) - \overline{e}\ \mathrm{div}(\rho\overline{\mathbf{V}})$ on $K$, which includes a possible upwinding $e_{\sigma,+}$ of the discrete internal energy: for $p \in X_{\mathscr{D}}$ and $e \in X_{\mathscr{D}}$,

$$\sum_{\sigma\in\mathscr{F}_K} e_{\sigma,+}\rho V_{K,\sigma}(p) - e_K \sum_{\sigma\in\mathscr{F}_K} \rho V_{K,\sigma}(p) = \sum_{\sigma\in\mathscr{F}_K} \rho V_{K,\sigma}(p)(e_{\sigma,+} - e_K).$$

We consider a time discretisation $(t^n)_{n=0,\dots,N}$ of the time interval $(0,\tau)$ with $t^0 = 0$ and $t^N = \tau$, and denote by $\delta t^{(n+\frac{1}{2})} = t^{n+1} - t^n$ the time step $n$. If $f = (f^n)_{n=0,\dots,N}$ is a family of functions, the discrete time derivative of $f$ is defined as

$$\delta_t^{(n+\frac{1}{2})} f = \frac{f^{n+1} - f^n}{\delta t^{(n+\frac{1}{2})}}.$$

We also set $\dot{\mathbf{u}} = (\dot{\mathbf{u}}^n)_{n=0,\dots,N}$ with $\dot{\mathbf{u}}^n = \frac{\mathbf{u}^n - \mathbf{u}^{n-1}}{t^n - t^{n-1}}$ and we write $\delta_t^{(n+\frac{1}{2})}\dot{\mathbf{u}} = 2\frac{\dot{\mathbf{u}}^{n+1} - \dot{\mathbf{u}}^n}{t^{n+1} - t^{n-1}}$. For given discrete pressures $p \in (X_{\mathscr{D}})^{N+1}$, temperatures $T \in (X_{\mathscr{D}})^{N+1}$ and displacement field $\mathbf{u} \in (\mathbf{U}_{\mathscr{D}})^{N+1}$, the discrete porosity $\phi = (\phi^n)_{n=0,\dots,N}$ and skeleton entropy $S_s = (S_s^n)_{n=0,\dots,N}$ are families of cellwise constant functions $\Omega \to \mathbb{R}$ on $\mathscr{M}$ such that $\phi^0, S_s^0$ are given (e.g., as projections of the continuous initial porosity and entropy) and, for all $n = 0, \dots, N-1$,

$$\begin{aligned}
\delta_t^{(n+\frac{1}{2})}\phi^n &= b\pi_{\mathscr{M}}(\delta_t^{(n+\frac{1}{2})}\mathrm{div}\mathbf{u}) - 3\alpha_\phi \delta_t^{(n+\frac{1}{2})}\Pi_{\mathscr{D}} T + \frac{1}{N}\delta_t^{(n+\frac{1}{2})}\Pi_{\mathscr{D}} p,\\
\delta_t^{(n+\frac{1}{2})}S_{s,\mathscr{D}} &= 3\alpha_s K_s \pi_{\mathscr{M}}(\delta_t^{(n+\frac{1}{2})}\mathrm{div}\mathbf{u}) - 3\alpha_\phi \delta_t^{(n+\frac{1}{2})}\Pi_{\mathscr{D}} p + \frac{C_s}{T_0}\delta_t^{(n+\frac{1}{2})}\Pi_{\mathscr{D}} T,
\end{aligned}$$

where $\pi_{\mathscr{M}}$ is the projection on piecewise constant functions on $\mathscr{M}$, that is, $(\pi_{\mathscr{M}} f)_{|K} = \frac{1}{|K|}\int_K f$ for all $K \in \mathscr{M}$.

We also define, for $\bullet = \{m, e\}$ and $n = 0, \dots, N-1$, the function $\widehat{h}_\bullet^{n+1} : \Omega \to \mathbb{R}$ as the piecewise constant function on $\mathscr{M}$ equal on $K \in \mathscr{M}$ to the average $\widehat{h}_{\bullet,K}^{n+1}$ of $h_\bullet$ on $(t^n, t^{n+1}) \times K$. The function $\widehat{\mathbf{h}}^{n+1} : \Omega \to \mathbb{R}^d$ is defined in the same way from $\mathbf{h}$.

Setting $\xi_K^n = \overline{\xi}(T_K^n)$ and $\xi_\sigma^n = \overline{\xi}(T_\sigma^n)$ for $\xi \in \{e, s\}$, the time stepping is defined by the discrete system:

$$\rho|K|\delta_t^{(n+\frac{1}{2})}\phi_K + \sum_{\sigma\in\mathscr{F}_K} \rho V_{K,\sigma}(p^{n+1}) = |K|\widehat{h}_{m,K}^{n+1} \qquad \forall K \in \mathscr{M}, \tag{3a}$$

$$\begin{aligned}
V_{K,\sigma}(p^{n+1}) + V_{L,\sigma}(p^{n+1}) &= 0 \qquad \forall \sigma = K|L \in \mathscr{F}^{\mathrm{int}},\\
V_{K,\sigma}(p^{n+1}) &= 0 \qquad \forall \sigma \in \mathscr{F}^{\mathrm{ext}}.
\end{aligned} \tag{3b}$$

$$\begin{aligned}
&|K|\Big(\delta_t^{(n+\frac{1}{2})}S_{s,K} + \rho\frac{\phi_K^n}{T_K^{n+1}}\delta_t^{(n+\frac{1}{2})}e_K\Big) + \frac{1}{T_K^{n+1}}\sum_{\sigma\in\mathscr{F}_K}\rho V_{K,\sigma}(p^{n+1})(e_{\sigma,+}^{n+1} - e_K^{n+1})\\
&+ \sum_{\sigma\in\mathscr{F}_K} G_{K,\sigma}(T^{n+1}) = |K|\left(\frac{\widehat{h}_{e,K}^{n+1}}{T_K^{n+1}} - \widehat{h}_{m,K}^{n+1}s_K^{n+1}\right) \qquad \forall K \in \mathscr{M}.
\end{aligned} \tag{3c}$$

$$\begin{aligned}
G_{K,\sigma}(T^{n+1}) + G_{L,\sigma}(T^{n+1}) &= 0 \qquad \forall \sigma = K|L \in \mathscr{F}^{\mathrm{int}},\\
G_{K,\sigma}(T^{n+1}) &= 0 \qquad \forall \sigma \in \mathscr{F}^{\mathrm{ext}}.
\end{aligned} \tag{3d}$$

$$\begin{aligned}
&\int_\Omega m_0(\delta_t^{(n+\frac{1}{2})}\dot{\mathbf{u}})\cdot\mathbf{v} + \int_\Omega \mathfrak{o}^e(\mathbf{u}^{n+1}) : \mathfrak{C}(\mathbf{v})\\
&- \int_\Omega \Big(b\Pi_{\mathscr{D}} p^{n+1} + 3\alpha_s K_s \Pi_{\mathscr{D}} T^{n+1}\Big)\mathrm{div}(\mathbf{v}) = \int_\Omega \widehat{\mathbf{h}}^{n+1}\cdot\mathbf{v} \qquad \forall \mathbf{v} \in \mathbf{U}_{\mathscr{D}}.
\end{aligned} \tag{3e}$$

Here, (3a)–(3b) discretise the mass conservation (1a), (3c)–(3d) discretise the entropy equation (2), and the mechanical equation (1c) is discretised by (3e). We note that, combining the mass and energy equations, the discretization of the term $\partial_t(\rho\overline{\phi}\overline{e}) + \mathrm{div}(\rho\overline{e}\overline{\mathbf{V}})$ is conservative. Note also that the discretization $\delta_t^{(n+\frac{1}{2})}\dot{\mathbf{u}}$ defined above is a natural extension of the classical formula $\frac{\mathbf{u}^{n+1} - 2\mathbf{u}^n + \mathbf{u}^{n-1}}{(\delta t)^2}$ in the case of a constant time step $\delta t$.

## 3 Energy estimate

Let us define the discrete Darcy and Fourier diffusive terms by

$$\mathfrak{D}(p^{n+1}) = \int_\Omega \frac{\mathbb{K}}{\mu} \nabla_{\mathscr{D}} p^{n+1} \cdot \nabla_{\mathscr{D}} p^{n+1}, \qquad \mathfrak{F}(T^{n+1}) = \int_\Omega \frac{\lambda}{T_0} |\nabla_{\mathscr{D}} T^{n+1}|^2,$$

and we assume that

$$M := \begin{bmatrix} \frac{1}{N} & -3\alpha_\phi \\ -3\alpha_\phi & \frac{C_s}{T_0} \end{bmatrix} \text{ is definite positive.}$$

The discrete energy is $\mathfrak{E} = (\mathfrak{E}^n)_{n=0,\dots,N}$ with $\mathfrak{E}^n : \Omega \to \mathbb{R}$ given by

$$\begin{aligned} \mathfrak{E}^n = \frac{1}{2} [\Pi_{\mathscr{D}} p^n \ \Pi_{\mathscr{D}} T^n] M \begin{bmatrix} \Pi_{\mathscr{D}} p^n \\ \Pi_{\mathscr{D}} T^n \end{bmatrix} + \rho \phi^n \Pi_{\mathscr{D}} e^n \\ + \frac{1}{2} \frac{E}{1+\nu} \left( |\mathbb{e}(\mathbf{u})|^2 + \frac{\nu}{1-2\nu} (\mathrm{div}\mathbf{u})^2 \right). \end{aligned}$$

Let us also set the discrete specific free enthalpy of the fluid as

$$g^{n+1} = \Pi_{\mathscr{D}} e^{n+1} + \frac{\Pi_{\mathscr{D}} p^{n+1}}{\rho} - \Pi_{\mathscr{D}} T^{n+1} \Pi_{\mathscr{D}} s^{n+1}.$$

Then, any solution of the discrete system (3) satisfies the following discrete energy estimate: for all $n = 0, \dots, N-1$,

$$\begin{aligned} \int_\Omega \frac{m_0}{2} \delta_t^{(n+\frac{1}{2})} |\dot{\mathbf{u}}|^2 + \int_\Omega \delta_t^{(n+\frac{1}{2})} \mathfrak{E} + \mathfrak{D}(p^{n+1}) + \mathfrak{F}(T^{n+1}) \\ \leq \int_\Omega \left( \widehat{h}_e^{n+1} + g^{n+1} \widehat{h}_m^{n+1} \right) + \int_\Omega \widehat{\mathbf{h}}^{n+1} \cdot \dot{\mathbf{u}}^{n+1}. \end{aligned}$$

To deduce a control on the primary discrete unknowns, we make the following assumptions.

- Throughout the simulation, $\phi \geq \phi_* > 0$; the model itself does not contain any mechanism that ensures that the continuous porosity remains positive, so this assumption is mandatory (see the introduction of [1]), but can also easily be checked during the simulation.
- The energy and entropy laws satisfy: $\overline{e}(\overline{T}) \geq 0$ for all $\overline{T}$, and $\overline{e} - \overline{T}\overline{s}$ is sub-quadratic in the sense that $\lim_{|\overline{T}| \to \infty} \frac{\overline{e}(\overline{T}) - \overline{T}\overline{s}(\overline{T})}{|\overline{T}|^2} = 0$.
- The mass, energy and momentum source terms $h_m, h_e, \mathbf{h}$ are bounded.
- The thermo-poro-elastic parameters satisfy $\frac{1}{N} > 0$, $C_s > 0$, $\alpha_\phi \geq 0$, $E > 0$, $\nu \in (0, \frac{1}{2})$.
- The specific average density satisfies $m_0 \geq m_* > 0$.

Then, using a discrete Gronwall lemma we can show that there exists $C$, depending only on the data, such that for all small enough maximum time step (such a condition is only needed if $\mathbf{h} \neq 0$), one has

$$\begin{aligned} \|\dot{\mathbf{u}}\|_{L^\infty(0,\tau;L^2(\Omega))} + \|\Pi_{\mathscr{D}} p\|_{L^\infty(0,\tau;L^2(\Omega))} + \|\Pi_{\mathscr{D}} T\|_{L^\infty(0,\tau;L^2(\Omega))} + \|\mathbf{u}\|_{L^\infty(0,\tau;H^1(\Omega))} \\ + \left\| \nabla_{\mathscr{D}} p \right\|_{L^2(0,\tau;L^2(\Omega))} + \|\nabla_{\mathscr{D}} T\|_{L^2(0,\tau;L^2(\Omega))} + \|\Pi_{\mathscr{D}} e\|_{L^\infty(0,\tau;L^1(\Omega))} \leq C. \end{aligned}$$

## 4 Numerical Validation

We investigate in this section the numerical convergence of the scheme based on the following analytical solution

$$\mathbf{u}(\mathbf{x},t) = 10^{-1}\mathrm{e}^{-t}\begin{pmatrix} x^2y^2 \\ -x^2y^2 \end{pmatrix},$$
$$p(\mathbf{x},t) = \mathrm{e}^{-t}\sin(x)\sin(y), \quad T(\mathbf{x},t) = \mathrm{e}^{-t}(2-\sin(x)\sin(y)),$$

on the domain $\Omega = (0,1)^2$ and time interval $(0,\tau)$ with $\tau = 1$. The fluid internal energy and entropy are defined by $\overline{e}(\overline{T}) = \overline{T}$ and $\overline{s}(\overline{T}) = \log(\frac{\overline{T}}{\overline{T}_0})$. Dirichlet boundary conditions are imposed for $p$, $T$ and $\mathbf{u}$ on $(0,\tau)\times\partial\Omega$ and the source terms $h_m$, $h_e$ and $\mathbf{h}$ are computed based on the data set defined in Table 1. The domain $\Omega$ is discretized using the first family of triangular meshes from [4] as illustrated in Figure 1. Each mesh indexed by $i \in \{1,2,3,4\}$ includes $\#\mathscr{M} = 56\times 4^{i-1}$ triangles. The HFV discretisation [3] of the flow and energy equations is combined with the $\mathbb{P}_2$ conforming Finite Element method for the mechanics to ensure the inf-sup condition and avoid potential oscillations of the pressure field at short times in the undrained regime. We consider a uniform time stepping of $(0,\tau)$ with time step $\Delta t = 10^{-4}$ chosen small enough to reduce the error due to the time discretization and focus on the convergence in space. The coupled nonlinear system is solved at each time step using a fixed-point method on cell pressures $p$ and temperatures $T$ accelerated by a Newton-Krylov algorithm [1]. At each iteration of the Newton Krylov algorithm, the $p,T$ sub-system is solved using a Newton Raphson algorithm and the contact mechanics is solved using a semi-smooth Newton method.

The $L^2$ space time errors for $p,T,\mathbf{u}$ and their gradients are exhibited in Tables (2)-(3)-(4) as functions of the mesh number $i$. Both the upwind and centered schemes are considered for the thermal convection as well as the two values of the permeability $\mathbb{K} = \mathbb{I}$ and $\mathbb{K} = 100\,\mathbb{I}$, respectively corresponding to equilibrated and convection dominated regimes. We first note that, due to the instability of the centered scheme in the convection dominated regime, this scheme fails to provide a solution for $\mathbb{K} = 100\,\mathbb{I}$ as a result of a failure of the nonlinear algorithm used to solve the scheme. Regarding the displacement field, second and first order convergence rates are observed in all cases for respectively $\mathbf{u}$ and $\nabla\mathbf{u}$. This is in accordance with the cellwise constant reconstruction $\Pi_{\mathscr{D}}$ of the pressure and temperature in the displacement field variational formulation (3e). The convergence rates for $p$ and $\nabla p$ are respectively roughly 1 and 2 in all cases as could be expected. On the other hand, the converge rates for $T$ and $\nabla T$ depend on the approximation of the convection term and on the convection diffusion regime. For equilibrated convection and diffusion, the centered scheme provides a higher convergence rate for $T$ (order 2, except on mesh 4 where the time error starts to dominate) than the upwind scheme (order between 1 and 2). An order 1 is observed on $\nabla T$ for both schemes. In the convection dominated regime, the upwind scheme exhibits a convergence rate slightly better than 1 for $T$ and an order roughly equal to 0.7 for $\nabla T$.

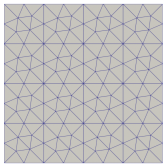

**Fig. 1.** Square domain $\Omega$ with its triangular mesh $i = 2$ using $56 \times 4$ cells.

**Table 1.** Material Properties

| Symbol | Quantity | Value | Unit |
|---|---|---|---|
| $E$ | Young modulus | 2.5 | Pa |
| $\nu$ | Poisson's coefficient | 0.25 | – |
| $N$ | Biot's modulus | 0.25 | $\mathrm{Pa}^{-1}$ |
| $b$ | Biot's coefficient | 1.0 | – |
| $K$ | Bulk modulus | 2.0 | Pa |
| $\mu$ | Fluid viscosity | 1.0 | Pa s |
| $\phi^0$ | Initial porosity | 4 | – |
| $\lambda$ | Effective thermal conductivity | 0.1 | $\mathrm{W\ m^{-1}\ K^{-1}}$ |
| $\rho$ | The fluid specific density | 1 | $\mathrm{Kg\ m^{-3}}$ |
| $3\alpha_s$ | The volumetric skeleton thermal dilation coefficient | 1 | $\mathrm{K}^{-1}$ |
| $3\alpha_\phi$ | The volumetric thermal dilation coefficient related to the porosity | 1 | $\mathrm{K}^{-1}$ |
| $T_0$ | Reference temperature | 1 | K |
| $m_0$ | Average fluid skeleton specific density | 0 | $\mathrm{Kg\ m^{-3}}$ |
| $C_s$ | The skeleton volumetric heat capacity | 0.5 | $\mathrm{J\ m^{-3}\ K^{-1}}$ |

**Table 2.** Errors and convergence rates obtained with the centered scheme using $\mathbb{K} = \mathbb{I}$.

| mesh | $P$ | | $\nabla P$ | | $T$ | | $\nabla T$ | | $U$ | | $\nabla U$ | |
|---|---|---|---|---|---|---|---|---|---|---|---|---|
| | Error | Rate | Error | Rate | Error | Rate | Error | Rate | Error | Rate | Error | Rate |
| 1 | 3.41E-03 | - | 7.40E-02 | - | 5.10E-04 | - | 7.40E-02 | - | 1.30E-02 | - | 5.17E-02 | - |
| 2 | 8.67E-04 | 1.97 | 3.68E-02 | 1.01 | 1.29E-04 | 1.98 | 3.68E-02 | 1.01 | 3.89E-03 | 1.74 | 2.41E-02 | 1.10 |
| 3 | 2.19E-04 | 1.99 | 1.84E-02 | 1.00 | 3.49E-05 | 1.89 | 1.84E-02 | 1.00 | 1.07E-03 | 1.86 | 1.15E-02 | 1.06 |
| 4 | 5.50E-05 | 1.99 | 9.17E-03 | 1.00 | 1.41E-05 | 1.31 | 9.18E-03 | 1.00 | 2.81E-04 | 1.93 | 5.62E-03 | 1.03 |

**Table 3.** Errors and convergence rates obtained with the upwind scheme using $\mathbb{K} = \mathbb{I}$.

| mesh | $P$ | | $\nabla P$ | | $T$ | | $\nabla T$ | | $U$ | | $\nabla U$ | |
|---|---|---|---|---|---|---|---|---|---|---|---|---|
| | Error | Rate | Error | Rate | Error | Rate | Error | Rate | Error | Rate | Error | Rate |
| 1 | 3.44E-03 | - | 7.40E-02 | - | 9.84E-04 | - | 7.93E-02 | - | 1.33E-02 | - | 5.11E-02 | - |
| 2 | 8.79E-04 | 1.97 | 3.68E-02 | 1.01 | 3.18E-04 | 1.63 | 3.93E-02 | 1.01 | 3.93E-03 | 1.76 | 2.39E-02 | 1.09 |
| 3 | 2.26E-04 | 1.96 | 1.84E-02 | 1.00 | 1.28E-04 | 1.31 | 1.96E-02 | 1.00 | 1.07E-03 | 1.87 | 1.15E-02 | 1.06 |
| 4 | 5.96E-05 | 1.92 | 9.17E-03 | 1.00 | 6.25E-05 | 1.03 | 9.81E-03 | 1.00 | 2.81E-04 | 1.93 | 5.62E-03 | 1.03 |

**Table 4.** Errors and convergence rates obtained with the upwind scheme using $\mathbb{K} = 100\,\mathbb{I}$.

| mesh | $P$ | | $\nabla P$ | | $T$ | | $\nabla T$ | | $U$ | | $\nabla U$ | |
|---|---|---|---|---|---|---|---|---|---|---|---|---|
| | Error | Rate | Error | Rate | Error | Rate | Error | Rate | Error | Rate | Error | Rate |
| 1 | 3.49E-03 | - | 7.40E-02 | - | 3.15E-02 | - | 6.24E-01 | - | 1.94E-02 | - | 8.12E-02 | - |
| 2 | 9.08E-04 | 1.94 | 3.68E-02 | 1.01 | 1.45E-02 | 1.12 | 3.84E-01 | 0.70 | 5.18E-03 | 1.91 | 3.64E-02 | 1.16 |
| 3 | 2.47E-04 | 1.88 | 1.83E-02 | 1.00 | 6.66E-03 | 1.12 | 2.38E-01 | 0.69 | 1.30E-03 | 1.99 | 1.63E-02 | 1.16 |
| 4 | 7.45E-05 | 1.73 | 9.17E-03 | 1.00 | 2.97E-03 | 1.16 | 1.48E-01 | 0.69 | 3.14E-04 | 2.05 | 7.16E-03 | 1.19 |

**Acknowledgments**: the authors would like to thank BRGM and Andra for partially supporting this work and authorizing its publication.

## References

1. Bonaldi, F., Brenner, K., Droniou, J., Masson, R., Pasteau, A., Trenty, L.: Gradient discretization of two-phase poro-mechanical models with discontinuous pressures at matrix fracture interfaces. ESAIM: Mathematical Modelling and Numerical Analysis, vol. 55, 5, pp. 1741-1777 (2021).
2. Coussy, O.: Poromechanics, John Wiley & Sons (2004).
3. Droniou, J., Eymard, R., Gallouët, T., Herbin, R.: A Unified approach to Mimetic Finite Difference, Hybrid Finite Volume and Mixed Finite Volume methods. Mathematical Models and Methods in Applied Sciences, vol. 20, 02, pp. 265-295 (2010).
4. Herbin, R., Hubert, F.: Benchmark on discretization schemes for anisotropic diffusion problems on general grids, in the Proceedings of the conference Finite volumes for complex applications V, Jun 2008, France. pp. 659-692.